

## Three-dimensional studies of the 1991/1992 northern hemisphere winter using domain-filling trajectories with chemistry

E. R. Lutman, J. A. Pyle, M. P. Chipperfield, D. J. Lary, and I.

Kilbane-Dawe

University of Cambridge, Centre for Atmospheric Science, Cambridge, England

J. W. Waters

Jet Propulsion Laboratory, California Institute of Technology, Pasadena

N. Larsen

Danish Meteorological Institute, Copenhagen, Denmark

**Abstract.** We describe a new and computationally efficient technique for global three-dimensional modeling of stratospheric chemistry. This technique involves integrating a photochemical package along a large number of independent trajectories to produce a Lagrangian view of the atmosphere. Although Lagrangian chemical modeling with trajectories is an established procedure, this extension of integrating chemistry along a large number of domain-filling trajectories is a novel technique. This technique is complementary to three-dimensional Eulerian chemical transport modeling and avoids spurious mixing caused by low resolutions or diffusive transport schemes in these models. We illustrate the technique by studying the chlorine activation in the Arctic winter lower stratosphere. A photochemical model was integrated along large ensembles of calculated trajectories between 20 and 100 mbar for the 1991/1992 winter in order to produce a three-dimensional chemical picture. Large amounts of chlorine was activated at low altitudes (80 to 100 mbar) as well as altitudes near 50 mbar. This activated air was well contained at all levels, with little indication of mixing into lower latitudes. Model results for early January 1992 were compared to daily Microwave Limb Sounder (MLS) ClO observations at 465 K. The structure and evolution of the activated chlorine was well reproduced, giving faith in the technique, although absolute modeled ClO amounts were smaller than the MLS data. A larger number of domain-filling isentropic trajectories were also run at 475 K to produce a higher-resolution picture of vortex evolution in late January 1992. The model successfully reproduced the wave breaking events which characterized this period causing transport of activated air to lower latitudes.

### Introduction

Severe ozone depletion has been observed in the Antarctic spring as a result of enhanced chlorine radicals produced when polar stratospheric clouds (PSCs) form in the cold polar vortex. A gradual decrease in total ozone has also been seen in the northern hemisphere from 1965 to 1986 [World Meteorological Organization (WMO), 1990]. In midlatitudes, 4 to 8% ozone decreases have been observed during the 1980s [Stolarski *et al.*, 1991]. The climatologies of the northern and southern hemispheres are significantly different. Arctic

dynamics are more variable leading to more distortions of the vortex, and temperatures are generally warmer than in the Antarctic, leading to fewer PSC occurrences. Despite these differences it is clear that the Arctic polar vortex is generally, at some stage of the winter, primed for ozone depletion. For example, observations from the Microwave Limb Sounder (MLS) onboard the Upper Atmosphere Research Satellite (UARS) show substantial chlorine activation in the 1991/1992 vortex [Waters *et al.*, 1993], as large as in the south.

Three dimensional modeling of stratospheric chemistry has made dramatic progress in recent years. Offline three-dimensional models, forced by meteorological analyses, are powerful tools for interpreting a wide range of atmospheric observations (for example Lefevre *et al.*, 1994). However, the high resolution needed by these models to faithfully reproduce the chemistry and

Copyright 1997 by the American Geophysical Union.

Paper number 96JD00698.  
0148-0227/97/96JD-00698\$09.00

dynamics of, for example, the polar region makes three-dimensional models costly to run and produces a large amount of output.

This study demonstrates a new technique which can be used to model stratospheric chemistry in three dimensions and in particular the polar vortex. Large ensembles of trajectories with chemistry are used to calculate the three-dimensional evolution of chemical fields. We illustrate the use of the technique by considering the evolution of enhanced active chlorine,  $\text{ClO}_x$  ( $= \text{Cl} + \text{ClO} + 2\text{Cl}_2\text{O}_2$ ), during December 1991 and January 1992. A day-by-day comparison of model  $\text{ClO}$  with MLS observations in early January is presented. A period when the vortex became disturbed in late January is investigated by using domain-filling trajectories to study possible transport of activated air to lower latitudes.

## Method

The first step in the procedure is to calculate the Lagrangian trajectories of a large number of particles in the region of interest. Then, given a chemical initialization, the chemical evolution along a single trajectory can be calculated using a chemical box model. A three-dimensional (height, latitude, longitude) chemical picture on a certain day can also be produced by integrating a large number of trajectories on particular levels. Using the ensemble of endpoints, a complementary picture to other Eulerian global chemical transport models is obtained.

This method has certain advantages over traditional Eulerian global models. There is no mixing between air parcels and the results are not dependent on problems with diffusion and artificial mixing associated with the resolution and advection schemes of some global models. The integrations are also cheaper than global model integrations, allowing sensitivity studies to be performed (for example *Lutman et al.* 1994).

Although the idea of modeling stratospheric chemistry along trajectories is well established (for example, *Austin et al.* 1987), running multiple trajectories with chemistry is a new approach to three-dimensional modeling. This technique is complementary to other state of the art approaches, such as contour advection (for example, *Waugh et al.* 1993), or domain-filling trajectories with no chemistry (for example, *Fisher et al.* 1993).

## Trajectory Calculations

The trajectories used in this study were calculated using a model described by *Chipperfield et al.* [1995]. We used European Centre for Medium-Range Weather Forecasts (ECMWF) analyzed winds with a spectral resolution of T42. We calculated both isentropic trajectories and full three-dimensional trajectories where the vertical motion was obtained from the ECMWF analyses. The three-dimensional trajectories used in the first section were integrated from November 26,

1991. The domain-filling 475 K isentropic trajectories used in the second section were integrated from December 23, 1991. Photochemical trajectory calculations in the stratosphere have not traditionally been run for longer than about 10 days, usually because of the isentropic approximation employed in trajectory calculations. However, *Sutton* [1994] has shown that the features revealed by long-duration, three-dimensional "domain-filling" trajectories, calculated after data assimilation of meteorological analyses, exhibit a coherent structure which agrees well with other, independently derived quantities, for example, potential vorticity.

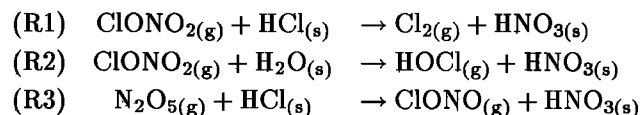
## Photochemical Models

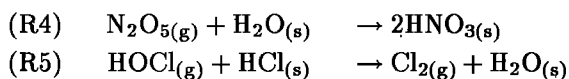
In this paper we have used two different chemical box models (model A and model B). Model A has a more detailed chemical scheme while model B is more computationally efficient, allowing more trajectories to be integrated. The two photochemical models are described below.

### Chemistry in Model A

The gas phase chemistry is, with the addition of bromine species, an extension of that used by *Lary and Pyle* [1991] and is described thoroughly by *Lary* [1991]. To save computational expense, the family approach is used in integrating the chemical tendencies. The chemical families included in the model are  $\text{O}_x$  ( $\text{O}(^1D) + \text{O}(^3P) + \text{O}_3$ ),  $\text{NO}_x$  ( $\text{N} + \text{NO} + \text{NO}_2 + \text{NO}_3$ ),  $\text{ClO}_x$  ( $\text{Cl} + \text{ClO} + 2\text{Cl}_2\text{O}_2$ ),  $\text{HO}_x$  ( $\text{H} + \text{OH} + \text{HO}_2$ ), and  $\text{Br}_x$  ( $\text{Br} + \text{BrO}$ ). The model also integrates separately the reservoir species  $\text{N}_2\text{O}_5$ ,  $\text{HNO}_3$ ,  $\text{HO}_2\text{NO}_2$ ,  $\text{H}_2\text{O}_2$ ,  $\text{ClONO}_2$ ,  $\text{HCl}$ ,  $\text{HOCl}$ ,  $\text{BrCl}$ ,  $\text{BrONO}_2$ ,  $\text{HBr}$ , and  $\text{OCIO}$  as well as some source gases ( $\text{N}_2\text{O}$ ,  $\text{H}_2\text{O}$  and  $\text{CH}_4$ ) and some CFCs. The gas phase photochemical and kinetic data are mostly taken from *DeMore et al.* [1990] unless otherwise stated. The time integration is performed using a fourth-order Runge-Kutta method with adaptive time step, after *Press et al.* [1992]. The model incorporates a detailed radiation scheme for the calculation of photolysis rates. A detailed treatment of diffuse radiation is included. The photolysis scheme is based on the work of *Meier et al.* [1982], *Nicolet et al.* [1982], and *Anderson* [1983], extended to describe the radiation field to zenith angles up to  $97^\circ$  [*Lary and Pyle*, 1991]. The temperature dependence of the  $\text{HNO}_3$  photolysis cross section [*Burkholder et al.*, 1994] is also included.

A detailed microphysical scheme *Larsen* [1991] is used to calculate PSC surface areas available for heterogeneous reactions based on *Toon et al.* [1989]. The following reactions are available on polar stratospheric clouds with specified sticking coefficients,  $\gamma$ , for type 1 PSCs taken from *WMO* [1990].





The reactions are treated as being of first order in the loss of the gaseous molecule. Reaction (R5) is included [Hanson and Ravishankara, 1991] and given the sticking coefficient suggested by Abbatt and Molina [1992] for “H<sub>2</sub>O-rich nitric acid trihydrate (NAT).” The reactions (R2) and (R4) also occur on sulphate aerosol in the model with an enhanced surface area outside the vortex and background values inside the vortex appropriate for 1991/1992. A sticking probability of 0.1 for reaction (R4) is used and the sticking probability for reaction (R2) is calculated as a function of temperature and reaches a maximum value of 0.1 at around 195 K [Hanson and Ravishankara, 1991].

### Chemical Initialization for Model A

Ideally, the individual trajectories should each use a unique chemical initialization appropriate for the starting location. Model B is initialized individually from three-dimensional model chemical fields (see later). However, with model A a simpler approach was adopted. Model A was initialized as shown in Table 1, according to an in- or out-of-vortex categorization of the trajectory starting points (judged by the steepest gradients in potential vorticity, [Braathen et al., 1992]). The trajectories were then integrated for a long period to overcome the effects of the crude initialization on the short-lived species. This approach is particularly suited to modeling chlorine activation since in the presence of PSCs the chlorine reservoirs react rapidly and so chemical initialization is not critical.

The values of total inorganic chlorine, Cl<sub>y</sub>, could be a little high. For example, Schmidt et al. [1994] calculated, using measurements of the chlorofluorocarbons (CFCs), only a little over 3 ppbv within the lower stratospheric polar vortex during the European Arctic Stratospheric Ozone Experiment (EASOE), while Oelhaf et al. [1994] measured 3.3 ppbv of ClONO<sub>2</sub> deep inside the vortex in mid-March 1992. This approach, in which only in- or out-of-vortex cases are considered,

will also oversimplify the structure on any particular surface. Nonetheless, it should allow us to identify the impact of processing by PSCs and aerosol, the main objective of this study.

### Chemistry in Model B

Model B uses the chemistry scheme from the TOMCAT three-dimensional CTM [Chipperfield et al., 1993]. It has a fairly detailed description of the O<sub>x</sub>, NO<sub>y</sub>, ClO<sub>y</sub>, BrO<sub>y</sub> and HO<sub>x</sub> families as well as longer-lived tracers (for example, CH<sub>4</sub> and N<sub>2</sub>O). PSCs are allowed to form in the model when the temperature drops below the threshold temperature according to Hanson and Mauersberger [1988]. Reactions (R2), (R4), and (R5) occur in the model on both PSCs and a volcanic sulphate aerosol distribution. The box model was initialized chemically according to three-dimensional chemical fields calculated for the starting day by the TOMCAT model. Model B has the advantage of being more computationally efficient (since it was designed for use in a three-dimensional model) and thus allows more trajectories to be integrated in a shorter time than model A. The main difference between model B and model A is that model B does not contain a microphysical scheme.

Note that the heterogeneous chemistry schemes in both models are based around the transformation from sulphate aerosol to NAT at a critical temperature. Recent ideas, including the possibilities of sulphuric acid tetrahydrate (SAT) or supercooled ternary solutions (STS), are not included here.

### Chemical Initialization for Model B

Model B was initialized directly from output of the three-dimensional TOMCAT model for the appropriate day.

### Meteorology of the 1991/1992 Winter

The meteorology of the 1991/1992 (EASOE) winter has been described in detail by Naujokat et al. [1993] and Farman et al. [1994]. The vortex formed between late November and early December at upper lev-

**Table 1.** Trajectory Initializations at Different Potential Temperature Levels Relative to the Vortex Edge (ppbv)

θ Level	400 K		475 K		550 K	
Position	In	Out	In	Out	In	Out
O <sub>x</sub>	2.4E+3	2.4E+3	2.4E+3	2.4E+3	2.4E+3	2.4E+3
H <sub>2</sub> O	5.0E+3	5.0E+3	5.0E+3	5.0E+3	5.0E+3	5.0E+3
CO	1.8E+1	1.8E+1	1.8E+1	1.8E+1	1.8E+1	1.8E+1
CH <sub>4</sub>	8.0E+1	6.0E+2	5.0E+2	1.0E+3	8.0E+1	8.0E+1
N <sub>2</sub> O	1.5E+1	1.1E+2	9.0E+1	1.9E+2	1.5E+1	1.1E+2
NO <sub>y</sub>	18.9	13.5	12.14	7.0	18.6	13.5
Cl <sub>x</sub>	0.2	0.2	0.2	0.2	0.2	0.2
ClONO <sub>2</sub>	0.4	0.4	0.4	0.4	0.4	0.4
HCl	2.3	2.3	2.7	2.3	2.3	2.3
Cl <sub>y</sub>	3.2	3.1	3.5	3.1	3.1	3.1
Br <sub>y</sub>	4.0E-3	4.0E-3	8.0E-3	8.0E-3	8.0E-3	8.0E-3

els. Temperatures dropped during late December and early January in the lower stratosphere. Temperatures were frequently low enough for PSC formation in the core of the jet stream [Farman *et al.* 1994], allowing a large amount of air to be processed heterogeneously. In this work the extent of the heterogeneous processing is investigated. A blocking ridge over the Atlantic and NW Europe affected the structure of the polar vortex which became distorted in late January with two distinct lobes of the vortex forming over Greenland and Europe. PSC processing stopped comparatively early in the winter due to a strong minor warming in late January.

## Results

### Evolution of $\text{ClO}_x$ in Late December and Early January using Model A

Model A, with its full microphysical scheme, was integrated along 1500 three-dimensional trajectories spread over the range of 20 to 100 mbar. We investigated the altitudinal distribution of  $\text{ClO}_x$  ( $\text{Cl} + \text{ClO} + 2\text{Cl}_2\text{O}_2$ ) from November 26, 1991 to mid-January 1992.

**December.** No chlorine enhancement was observed in early December. This is in contrast to measurements by MLS [Waters *et al.*, 1993] which observed moderately enhanced ClO from December 7, 1991, onwards with high values notably around December 14, 1991. An increase in chlorine due to PSC processing was also calculated by Douglass *et al.* [1993] in a three-dimensional model simulation of early December. However, the critical temperature they assumed for PSC formation was about 2 K warmer than that calculated by Hanson and Mauersberger [1988]. These temperatures were used to "compensate for a slight warm bias in the assimilation temperature fields." The Hanson and Mauersberger [1988] critical temperature may anyway be too high [Carslaw *et al.*, 1994]. However, in situ measurements on the ER-2 aircraft [Toohey *et al.*, 1993] showed only slightly enhanced ClO on December 12, 1991 (with a maximum of 0.4 ppbv at 20 km at 65°N). The absence of enhanced ClO in the trajectory model integrations suggests either that the heterogeneous chemistry scheme is inappropriate; that the trajectories missed the areas of cold temperatures, or that small variations in temperature causing PSCs to form were missed by the ECMWF temperature analyses. By December 14 (not shown) our integrations contained a few points of enhanced chlorine (0.7 ppbv), although the majority of trajectories did not show any activation.

By December 27 the situation had changed considerably. Areas of enhanced active chlorine ( $\text{ClO}_x$ ) are calculated at all altitudes, with most of the high  $\text{ClO}_x$  situated between 40 and 80 mbar but a few points over 0.5 ppbv between 80 and 100 mbar. At 40 to 60 mbar (Plate 1) a large area of high chlorine was situated over the Arctic and extending over Russia (see figure caption for an explanation of how the figure is constructed). Large areas of chlorine over 0.5 ppbv are found with some points greater than 1 ppbv.

**January.** The  $\text{ClO}_x$  evolution during January is presented in Plate 2 between 40 and 100 mbar for January 5, 12, and 22. Note that because of descent of the three-dimensional trajectories over the course of the run, the resolution of the picture was degraded by January 22 (see figure caption). The highest values of 2 ppbv are produced at 40 to 60 mbar inside the vortex on January 5. Note that considerable amounts of activation were produced at low altitudes (the 80 to 100 mbar level). The area of high activation is well contained at all levels, with little indication of mixing into lower latitudes even at low altitudes. No evidence is seen of the activated chlorine observed by Waters *et al.* [1993] outside the vortex (Figure 1).

Although the number of trajectories used to construct Plate 2 is limited, the apparent containment of the vortex at low altitudes is consistent with the contour advection studies of Norton and Chipperfield [1996]. They showed that large interannual variability occurs in the mass of vortex air transported to lower latitudes. During 1991/1992 the vortex was well contained except for an event at 475 K in late January (see below).

By January 22, 1992, the vortex at 475 K and 550 K developed into a "kidney" shape [Braathen *et al.*, 1992], with one arm extending over northern Canada and the other extending over Russia. The highest  $\text{ClO}_x$  mixing ratios between 60 and 80 mbar reflect this behavior and hence are contained within the vortex. Highly activated air is seen over the Caspian Sea (Plate 2). The distortion of the vortex on January 22 at all levels means there is highly activated air at low latitudes inside the vortex, where photolysis rates are faster. However, the net ozone loss integrated along the trajectories on January 22 (not shown) does not show large loss inside the vortex. There is no net ozone loss on January 22 greater than 15% inside the vortex despite the high levels of ClO. This is because the simultaneous presence of activated chlorine and exposure to sunlight only occurs for a short time; there is rapid instantaneous ozone loss in late January which is halted by the decay of  $\text{ClO}_x$ .

There is no evidence in these runs of activated air breaking off the vortex near 180°E around January 20 as indicated by other trajectory runs and other studies (see higher-resolution trajectory studies performed for this period below).

### Evolution of ClO From January 5 to 13, 1992

The period January 5 to 13, 1992, is investigated in further detail in this section. The evolution of ClO in the lower stratosphere calculated from the trajectory integrations is compared to measurements by MLS [Waters *et al.*, 1993]. The ClO measured by MLS is presented at 465 K at approximately local noon (Figure 1). Since ClO has a large diurnal cycle, comparison between model ClO at 1200 UT and ClO measured at local noon is unsatisfactory. For this reason the model ClO is also presented every day at approximately local noon (Plate 3).

To compare with the version 3 MLS data on the 465 K potential temperature level (Figure 1), modeled ClO is presented in Plate 3 for the range 425 to 500 K (this

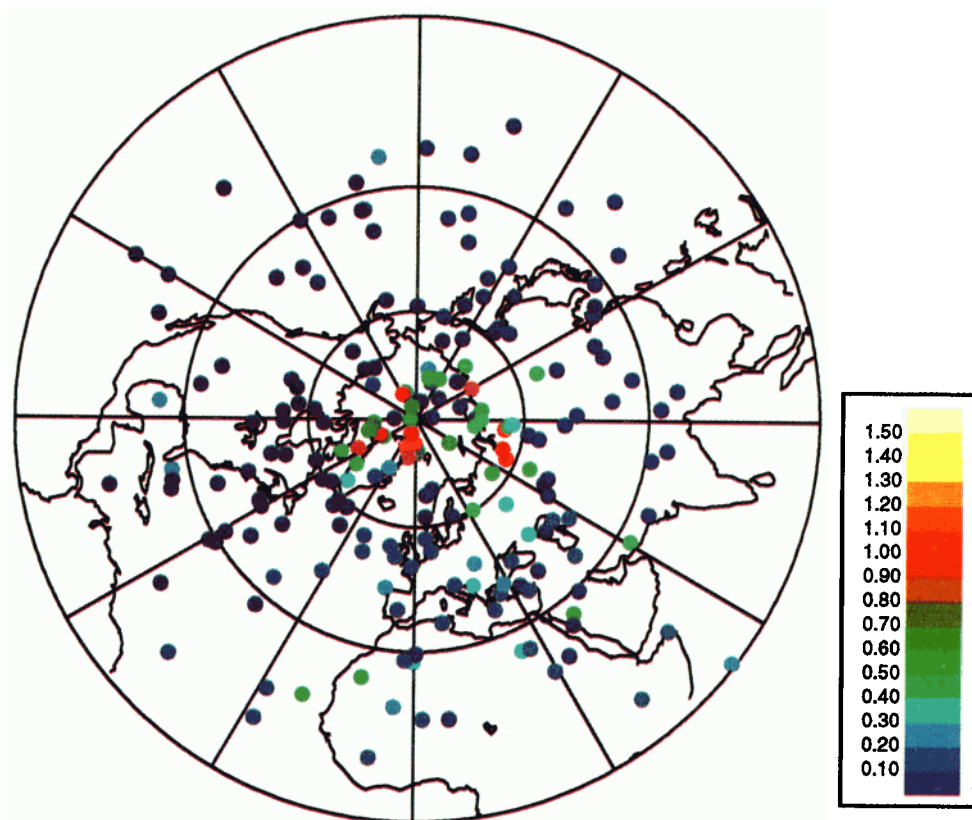


**Plate 1.**  $\text{ClO}_x$  (ppbv) on December 27, 1991, at 40 to 60 mbar calculated using model A. The  $\text{ClO}_x$  values are shown at the location of the individual trajectories.

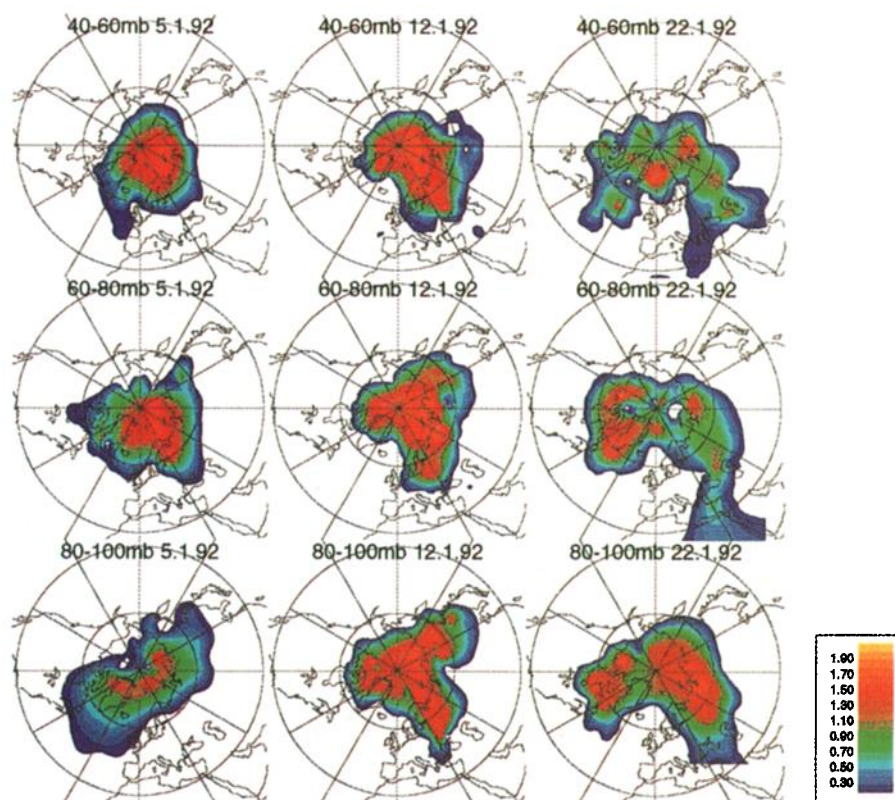


**Plate 2.** Time and altitude variation of  $\text{ClO}_x$  (ppbv) from model A during January 1992 projected onto three pressure intervals. First row;  $P = 40$  to  $60$  mbar. Second row;  $P = 60$  to  $80$  mbar. Third row;  $P = 80$  to  $100$  mbar. Days presented are January 5, 12, and 22, 1992. Because of descent during the course of the run, there are approximately 100 trajectory endpoints per plot on January 22, 1992, compared to approximately 200 endpoints per plot on January 12, 1992. The  $\text{ClO}_x$  field is calculated by projecting the  $\text{ClO}_x$  taken from the trajectory end points onto a single level and interpolating between the end points.

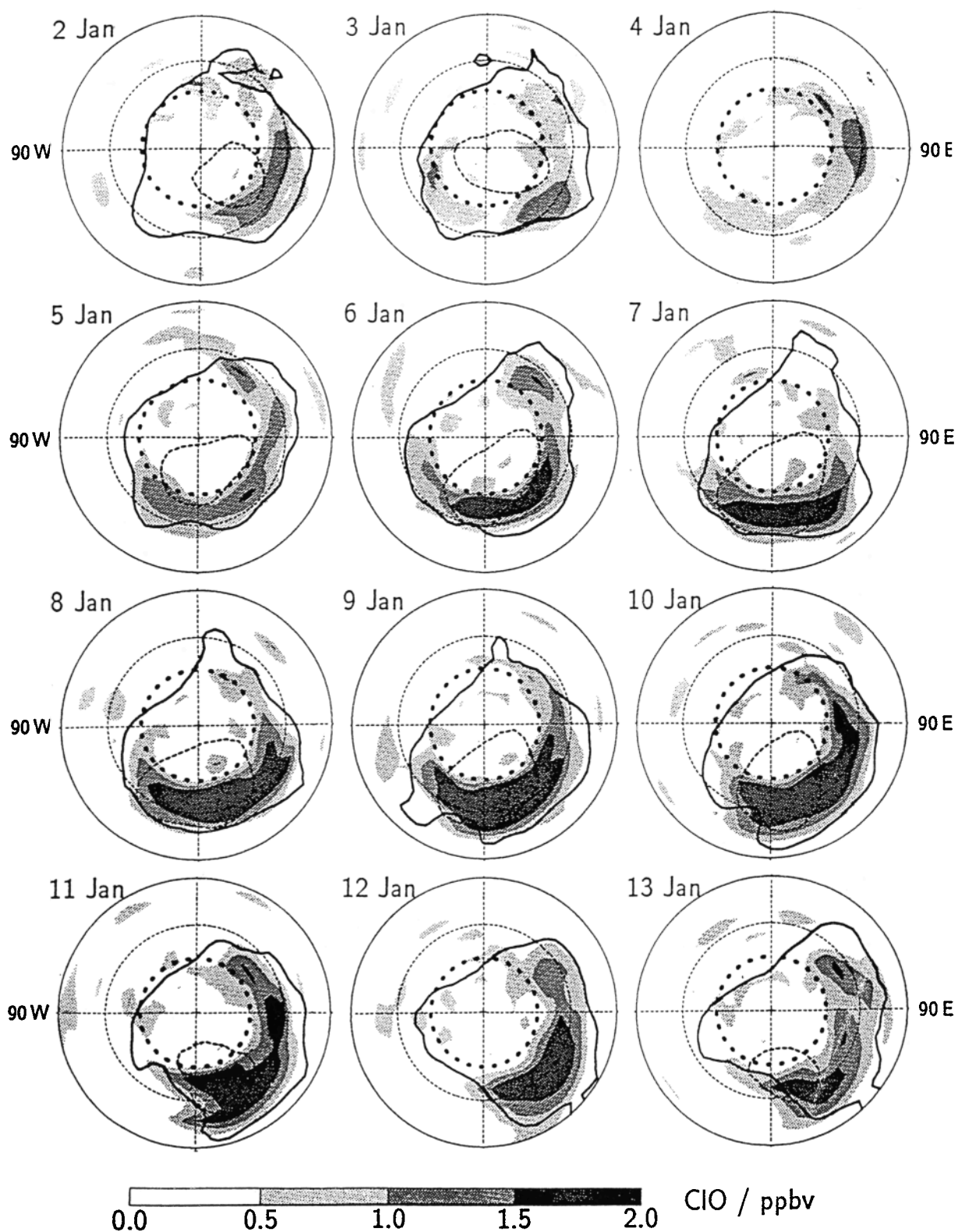


**Figure 1.** Microwave Limb Sounder version 3 ClO (ppbv) between January 2 and 13, 1992, at 465 K. (Figure taken from *Waters et al.* [1993]).



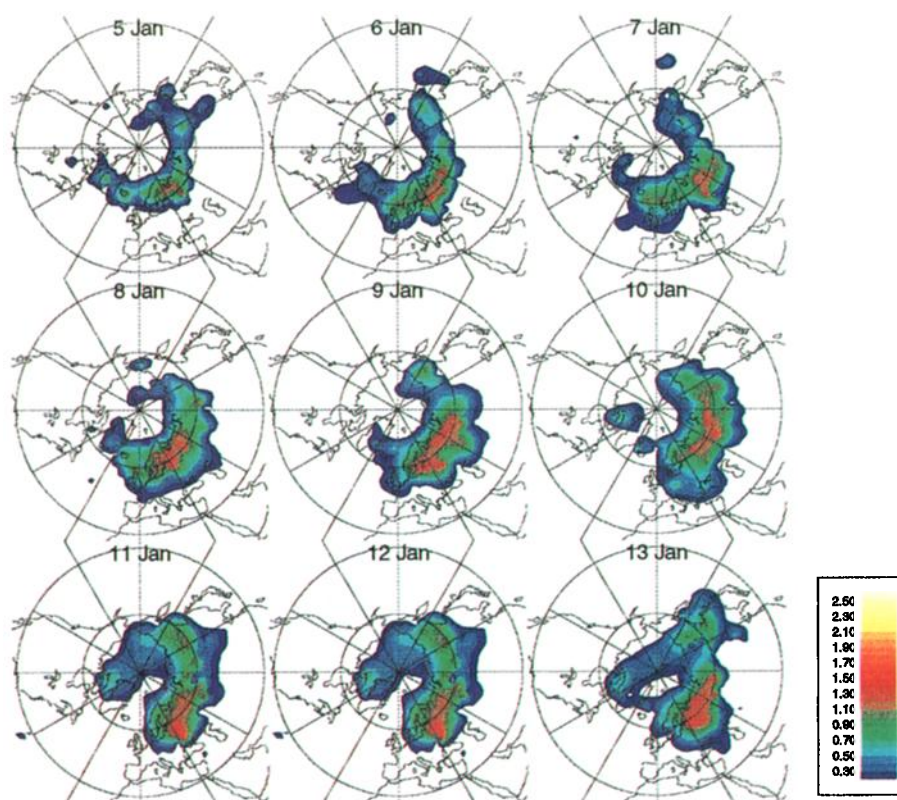


**Plate 3.** ClO (ppbv) calculated using model A between January 5 and 13, 1992, for 425 to 500 K at local noon. There are approximately 290 trajectory endpoints per plot.

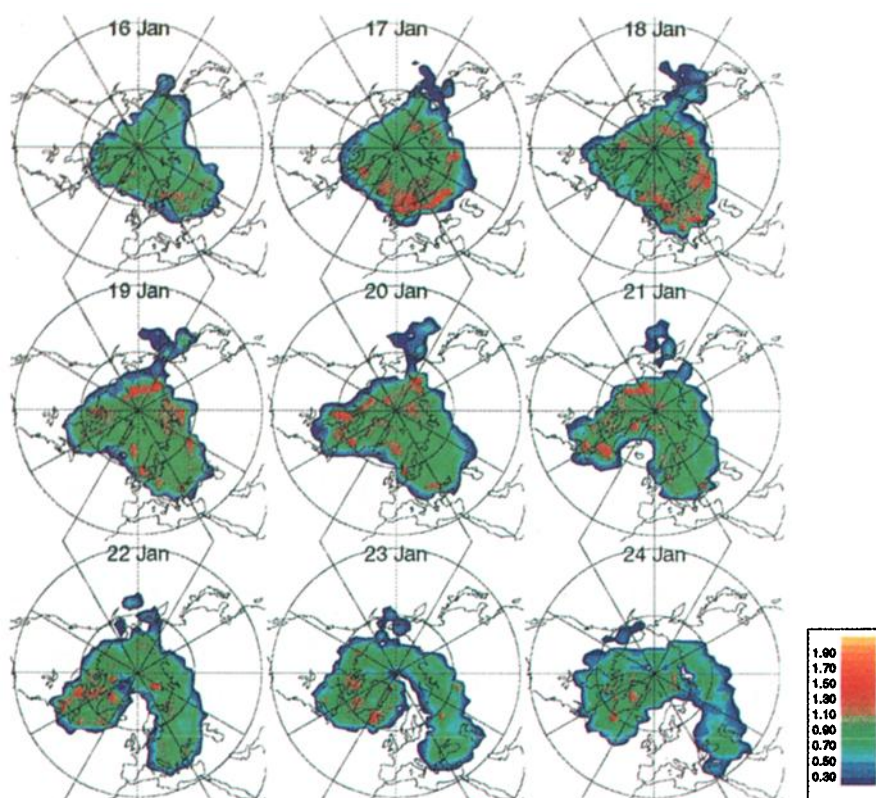


**Plate 4.** ClO<sub>x</sub> (ppbv) at 475 K for January 16 to 24, 1992, using chemical model B. There are 1280 endpoints per plot.

range is used to obtain an adequate number of data points, approximately 290 points, per figure). On most of the days shown, the shape of the area of the modeled maximum CIO is remarkably similar to that of MLS although the absolute magnitudes are lower. It should be noted that the magnitude of the version 3 CIO data shown in Figure 1 needs to be reduced by 8% (J.W. Waters, personal communication, 1995); see errors discussion below. The structure inside the region of enhanced CIO is also well reproduced. From January 5 the areas of maximum model CIO and maximum MLS CIO increase in size. On some days the MLS CIO extends farther west than the maximum model CIO (although some enhanced CIO is still present). The reason for this is uncertain. It may be due to the overall levels of enhanced chlorine being smaller in the model than in the measurements. It may also be due to the error in output times as described in the errors discussion below. Alternatively, a warm bias in the ECMWF temperatures could mean the model misses some PSC regions. There are cold areas west of the activated chlorine, which may explain why MLS CIO extends farther west than the calculated CIO (see errors discussion below).

From January 9, 1992, the area of enhanced CIO observed by MLS moved to the east; this is also seen in the calculated CIO. The area of high CIO remains displaced to the east for the remainder of the period of investigation in both the model and the MLS CIO maps and the calculated CIO reproduces the structure of the MLS CIO extremely well during the remainder of the integration. For example, on January 11 in both cases the highest values of CIO are found around 20°E. There is a secondary maximum in both cases from 90°E, extending across the pole, due to thermal decomposition of the dimer, and also a small patch of CIO around 270°E in both cases.

The qualitatively good agreement in terms of location and evolution of the features in the modeled CIO fields and the MLS data gives confidence that the technique of domain-filling trajectories with chemistry can be used to generate three-dimensional chemical fields. The model also agrees well with the high-resolution ( $2^0 \times 2^0$ ) simulations of *Lefevre et al.* [1994] during the same period. This has been achieved by integrating chemistry in effectively only 290 boxes compared with  $180 \times 90$  needed for a single-level Eulerian  $2^0 \times 2^0$  model. As the trajectories evolve independently, reducing the number does not degrade the chemical evolution of those that remain, unlike reducing the number of grid boxes in an Eulerian model. *Chipperfield et al.* [this issue] compare results from domain-filling trajectories with high-resolution Eulerian model and also find that the trajectory calculations produce consistent features.

#### Sources of Error Present in MLS and in the Model

In this section we mention some sources of error present in the version 3 MLS CIO, and sources of error in the model which will affect this comparison.

There are some problems with the absolute values of the version 3 MLS CIO data set. As previously men-

tioned, the magnitude of the version 3 MLS CIO shown in Figure 1 is overestimated and needs to be reduced by 8%. (J.W. Waters, personal communication, 1995). The MLS CIO data values may also be a little too high in areas below the PSC temperature threshold, because of an incorrect treatment of the  $\text{HNO}_3$  in these areas.

There is some degree of error present in both the MLS and the model output times. The local solar times of the MLS measurements vary with latitude due to the precession of the satellite's orbit. Some small error may be present in both the absolute value of the model CIO and its precise location since the model does not output CIO at exactly local noon. This is because, for the large number of trajectories being processed, data are output by the model at a constant time step (to limit model output). Thus the CIO concentration is selected from each trajectory when the end of the time step falls at some local time between 1200 and 1259 LT. The maximum possible error in the output time is  $1/24 \text{ day} = 0.0417 \text{ day}$ . The possible error in CIO near local noon due to this maximum variation of 0.0417 day is very small. The variation in longitude may be somewhat larger, a possible maximum error in longitude at these high latitudes (around 70°N) is estimated as between 1° and 3°. The error in latitude is expected to be considerably smaller.

So far, our comparison between model and MLS data has been only qualitative. A quantitative comparison between model and MLS CIO would be hindered by the errors mentioned above, and since in this work we are describing a novel technique, and illustrating it with MLS data, a quantitative comparison is not included.

#### Vortex Distortion in Late January 1992 Using Model B

There is currently much debate concerning the mechanisms responsible for midlatitude ozone loss. Possible causes may include in situ loss due to chlorine activation on sulphuric acid aerosol, or loss due to a temporary displacement of the vortex bringing air with enhanced chlorine over mid latitudes. Alternatively air with enhanced chlorine may be expelled from the vortex (the "flowing-processor" theory), particularly during times of distortion, or from low altitudes where the vortex is less well contained.

In mid-January the lower stratospheric vortex as shown by ECMWF analyses was a single, coherent entity, slightly disturbed by planetary waves. By January 20 a ridge over the Northeast Atlantic Ocean, associated with persistent tropospheric blocking, had distorted the vortex. The ridge continued to develop and the analyses show the development of two distinct vortex centers. The ECMWF analyses indicate that the vortex regained its initial coherence after January 24.

Vortex distortion makes exchange of vortex air with midlatitudes highly probable. Since exchange of air between vortex and midlatitudes is one possible cause of midlatitude ozone loss; this period was examined in more detail using model B. This model was used since it is more computationally efficient and allows a higher number of trajectories to be run, increasing the spatial



resolution of the results. The possible expulsion of activated air and intrusion of midlatitude air during this highly unstable period was investigated.

The 1280 isentropic trajectories were run at 475 K in this study, concentrated in middle and high latitudes. The forward trajectories were started on a grid from 80°N to 30°N (excluding 70°N) at a resolution of 5° and at a longitude interval of every 2.81°. The results may be compared to Plate 2. Because of the much larger number of trajectories used in this integration, the results are at a higher spatial resolution than shown in Plate 2.

ClO<sub>x</sub> taken from the trajectories is plotted for January 1992 at 475 K (Plate 4). The vortex is full of activated air, with values of up to 1.4 ppbv. From January 17 at about 150°E, activated ClO<sub>x</sub> is seen outside the vortex. During the whole period of the integration the "blob" of highly activated air remained near the edge of the vortex around 180°E. This streamer was also observed by *Waugh et al.* [1994] who used high-resolution contour advection with surgery (CAS). The blob remained in high latitudes, and the activated chlorine relaxed back to background levels. This blob of activated air was not seen in Plate 2. The area of the activated air inside the vortex began to distort on January 19, 1992, and this distortion increased over the next few days with one limb extending over Greenland and Canada and the other limb extending over the European sector. By January 20 the activated air had distorted into a kidney shape. The limb over the European sector extended further on 21 January and on January 22 to 23, low activated air appeared to be entrained into the vortex between the two limbs. The entrainment feature was also reported by *Pyle et al.* [1994]. This feature was not seen in Plate 2, our low-resolution run, again being missed by the fewer (three-dimensional) trajectories. *Plumb et al.* [1994] used CAS to estimate that the vortex in late January included a few percent of intruded air following this event.

## Conclusions

We have described a new approach to three-dimensional global chemical modeling consisting of integrating a photochemical box model along a large number of domain-filling trajectories. This procedure provides a three-dimensional Lagrangian picture of the atmosphere which complements that obtained from a traditional three-dimensional Eulerian model. Moreover, this technique avoids some problems associated with low-resolution Eulerian models concerned with spurious numerical diffusion and excess mixing between grid boxes.

We have illustrated the technique of domain-filling trajectories with chemistry by studying chlorine activation in the Arctic lower stratosphere. A photochemical model was integrated along multiple / domain-filling trajectories during the 1991/1992 northern hemisphere

winter. Results from the model were compared to MLS ClO observations during early January. The model reproduced the location and evolution of ClO very well providing support for the fidelity of the technique.

The results (presented in Plates 2 and 4) show little indication of the vortex acting as a processor. Considerable active chlorine is produced at low altitudes; however, it does not appear to be exported to midlatitudes. When the vortex undergoes a major distortion (Plate 4), modest amounts of air appear to be exported. This is in agreement with high-resolution dynamical studies contour advection studies [*Waugh et al.*, 1994].

Despite the length of the trajectories being longer than that generally considered to be ideal (approximately 10 days), their behavior was consistent with meteorological analyses. The density of trajectories required to reconstruct an adequate picture of the atmosphere depends on the meteorological situation. While a medium resolution run reproduced the observed MLS ClO well when the vortex was stable in early January, during an unstable period, such as late January 1992, the number of trajectories must be increased to achieve an adequate picture. In our experiments we increased the number of trajectories by a factor of 10.

The domain-filling trajectories with the chemistry method is a novel approach complementary to running global transport models. In a Lagrangian run the resolution of the chemical picture is dependent only on the number of trajectories which are run and the interpolation between the endpoints for graphical display. The high resolution of the chemical picture which may be obtained by running many trajectories is ideal for examining highly detailed structures such as vortex distortions. They are a useful and inexpensive way of modeling the chemical evolution of the winter, allowing sensitivity studies to be performed much more easily than in three-dimensional models (for example, *Lutman et al.*, 1994).

**Acknowledgments.** This work was funded by DG XII of the CEC under contract STEP-CT91-0139 for the support of EASOE. ERL was generously supported by NERC and a Gassiot Award from the Meteorological Office. IK-D was funded by the Human Capital and Mobility Programme (HCMP) proposal ERB4001GT921327. The modeling work described here is part of our UK NERC supported UGAMP effort. ERL would like to thank A.R. MacKenzie for all his help in the preparation of this paper.

## References

- Abbatt, J. P. D. and M. J. Molina, The heterogeneous reaction of HOCl + HCl Cl<sub>2</sub> + H<sub>2</sub>O on ice and nitric acid trihydrate: Reaction probabilities and stratospheric implications, *Geophys. Res. Lett.*, **19**, 461-464 1992.
- Anderson, D. E., The troposphere to stratosphere radiation field at twilight: A spherical model, *Planet. Space Sci.*, **31**, 1517-1523, 1983.
- Austin, J., R. C. Pallister, J. A. Pyle, A. F. Tuck, and A. M. Zavody, Photochemical model comparisons with LIMS observations in a stratospheric trajectory coordinate system, *Q. J. R. Meteorol. Soc.*, **113**, 361-392, 1987.

- Braathen, G. O., F. Stordal, T. Gunstrom, B. Knudsen, and K. Kloster, EASOE meteorology report, *Norw. Inst. for Air Res.*, Kjeller, Norway, 1992.
- Burkholder, J. B., R. K. Talukdar, A. R. Ravishankara, and S. Solomon, Temperature dependence of the  $\text{HNO}_3$  UV absorption cross sections, *J. Geophys. Res.*, **98**, 22,937-22,948, 1994.
- Carslaw, K. S., B. P. Luo, S. L. Clegg, T. Peter, P. Brimblecombe, and P. J. Crutzen, Stratospheric aerosol growth and  $\text{HNO}_3$  gas-phase depletion from coupled  $\text{HNO}_3$  and water-uptake by liquid particles, *Geophys. Res. Lett.*, **21**, 2479-2482, 1994.
- Chipperfield, M. P., D. Cariolle, P. Simon, R. Ramaroson, and D. J. Lary, A three-dimensional modeling study of trace species in the Arctic lower stratosphere during winter 1989-1990, *J. Geophys. Res.*, **98**, 7199-7218, 1993.
- Chipperfield, M. P., J. Kettleborough, and A. Pardaens, The TOPCAT offline trajectory model, *internal report of the UK Universities Global Atmos. Model. Proj.*, Cambridge, UK, 1995.
- Chipperfield, M. P., E. R. Lutman, J. Kettleborough, J. A. Pyle, and A. E. Roche, Model studies of chlorine deactivation and formation of  $\text{ClONO}_2$  collar in the Arctic polar vortex, *J. Geophys. Res.*, this issue.
- DeMore, W. B., M. J. Molina, S. P. Sander, D. M. Golden, R. F. Hamson, M. J. Kurylo, C. J. Howard, and A. R. Ravishankara, Chemical kinetics and photochemical data for use in stratospheric modeling, in *Evaluation 9, NASA JPL Publ. 90-1*, 1990.
- Douglass, A., R. Rood, J. Waters, L. Froidevaux, W. Read, L. Elson, M. Geller, Y. Chi, M. Cerniglia, and S. Steenrod, A three-dimensional simulation of the early winter distribution of reactive chlorine in the north polar vortex, *Geophys. Res. Lett.*, **20**, 1271-1274, 1993.
- Farman, J. C., A. O'Neill, and R. Swinbank, The dynamics of the Arctic polar vortex during the EASOE campaign, *Geophys. Res. Lett.*, **13**, 1195-1198, 1994.
- Fisher, M., A. O'Neill, and R. Sutton, Rapid descent of mesospheric air into the stratospheric polar vortex, *Geophys. Res. Lett.*, **20**, 1267-1270, 1993.
- Hanson, D. R., and K. Mauersberger, Vapour-pressures of  $\text{HNO}_3/\text{H}_2\text{O}$  solutions at low temperatures, *J. Phys. Chem.*, **92**, 6167-6170, 1988.
- Hanson, D. R., and A. R. Ravishankara, The reaction probabilities of  $\text{ClONO}_2$  and  $\text{N}_2\text{O}_5$  in 40 to 75% sulphuric acid solutions, *J. Geophys. Res.*, **96**, 17,307-17,314, 1991.
- Larsen, N., Polar stratospheric clouds: A microphysical simulation model, *Dan. Meteorol. Inst. Sci. report*, 1991-92, Copenhagen, 1991.
- Lary, D. J., Photochemical studies with a three-dimensional model of the atmosphere, *Ph.D. thesis, University of Cambridge*, Cambridge, 1991.
- Lary, D. J., and J. A. Pyle, Diffuse radiation, twilight and photochemistry I, *J. Atmos. Chem.*, **13**, 373-392, 1991.
- Lefevre, F., G. P. Brasseur, I. Folkins, A. K. Smith, and P. Simon, Chemistry of the 1991-1992 stratospheric winter: Three-dimensional model simulations, *J. Geophys. Res.*, **99**, 8183-8195, 1994.
- Lutman, E. R., J. A. Pyle, D. J. Lary, A. R. MacKenzie, I. Kilbane-Dawe, R. L. Jones, N. Larsen, and B. Knudsen, Trajectory model studies of  $\text{ClO}_x$  activation and ozone loss during the 1991/92 northern hemispheric winter, *Geophys. Res. Lett.*, **13**, 1419-1422, 1994.
- Meier, R. R., D. E. Anderson, and M. Nicolet, Radiation field in the troposphere and stratosphere from 240 to 1000nm, *Gen. Anal. Planet. Space Sci.*, **30**, 923, 1982.
- Naujokat, B., et al., The stratospheric winter 1991/92, *Beil. Berl. Wetterkarte*, **SO 18/92**, 1993.
- Nicolet, M., R. R. Meir, and D. E. Anderson, The radiation field in the troposphere and stratosphere from 240 - 1000nm: Numerical analysis, *Planet. Space Sci.*, **30**, 935-983, 1982.
- Norton, W. A., and M. P. Chipperfield, Quantification of the transport of chemically activated air from the northern hemisphere polar vortex, *J. Geophys. Res.*, **100**, 25,817, 1996.
- Oelhaf, H., T. v. Clarmann, H. Fischer, F. Friedl-Vallon, C. Fritzsche, A. Linden, C. Piesche, M. Seefeldner, and W. Volker, Stratospheric  $\text{ClONO}_2$  and  $\text{HNO}_3$  profiles obtained inside the Arctic vortex from MIPAS-B limb emission spectra obtained during EASOE, *Geophys. Res. Lett.*, **21**, 1263-1266, 1994.
- Plumb, R. A., D. W. Waugh, R. J. Atkinson, P. A. Newman, L. R. Lait, M. R. Schoeberl, E. V. Browell, A. J. Simmons, and M. Lowenstein, Intrusions into the lower stratospheric Arctic vortex during the winter of 1991-1992, *J. Geophys. Res.*, **99**, 1089-1105, 1994.
- Press, W. H., S. A. Teukolsky, W. T. Vetterling, and B. P. Flannery, *Numerical recipes in FORTRAN - The art of scientific computing*, 2nd ed., Cambridge Univ. Press, New York, 1992.
- Pyle, J. A., G. D. Carver, and U. Schmidt, Some case studies of chlorine activation during the EASOE campaign, *Geophys. Res. Lett.*, **13**, 1431-1434, 1994.
- Schmidt, U., R. Bauer, A. Engel, R. Borchers, and J. Lee, The variation of available chlorine,  $\text{ClO}_y$ , in the Arctic polar vortex derived from regular profile observations of  $\text{CCl}_2\text{F}_2$  (CFC 12) during EASOE, *Geophys. Res. Lett.*, **13**, 1215-1218, 1994.
- Stolarski, R. S., D. Bloomfield, R. D. McPeters, and J. R. Herman, Total ozone trends deduced from Nimbus 7 TOMS data, *Geophys. Res. Lett.*, **18**, 1015-1018, 1991.
- Sutton, R., Lagrangian flow in the middle atmosphere, *Q. J. R. Meteorol. Soc.*, **120**, 1299-1321, 1994.
- Tooney, D. W., L. M. Avallone, L. R. Lait, P. A. Newman, M. R. Schoeberl, D. W. Fahey, E. L. Woodbridge, and J. G. Anderson, The seasonal evolution of reactive chlorine in the northern hemisphere stratosphere, *Science*, **261**, 1134-1135, 1993.
- Toon, O. B., R. P. Turco, J. Jordan, J. Goodman, and G. F. Fehsenfeld, Physical processes in polar stratospheric ice clouds, *J. Geophys. Res.*, **94**, 11,359-11,380, 1989.
- Waters, J. W., L. Froidevaux, W. G. Read, G. L. Manney, L. S. Elson, D. A. Flower, R. F. Jarnot, and R. S. Harwood, Stratospheric  $\text{ClO}$  and ozone from the Microwave Limb Sounder on the Upper Atmosphere Research Satellite, *Nature*, **362**, 597-602, 1993.
- Waugh, D. W., Contour surgery simulations of a forced polar vortex, *J. Atmos. Sci.*, **50**, 714-730, 1993.
- Waugh, D. W., et al., Transport out of the lower stratospheric arctic vortex by Rossby-wave breaking, *Geophys. Res.*, **99**, 1071-1088, 1994.
- World Meteorological Organization (WMO), Scientific assessment of stratospheric ozone: 1990, *Global Ozone Res. and Monit. Project WMO Rep. 21*, Geneva, 1990.

M. P. Chipperfield, I. Kilbane-Dawe, D. J. Lary, E. R. Lutman, and J. A. Pyle, University of Cambridge, Centre for Atmospheric Science, Department of Chemistry, Lensfield Road, Cambridge, CB2 1EW, UK

N. Larsen, Danish Meteorological Institute, Lyngbyvej 100, DK-2100 Copenhagen O, Denmark.

J. W. Waters, Jet Propulsion Laboratory, California Institute of Technology, Pasadena, CA 91109

(Received September 2, 1995; revised February 21, 1996; accepted September 21, 1996.)